ACCEPTED MANUSCRIPT

Analysis of urban development on land cover changes of three cities of Gujarat state, India

Alpesh M. Patel, Anil Suthar

DOI: 10.5937/gp26-39440

To appear in: Geographica Pannonica
Received Date: 31 July 2022
Revised Date: 26 October 2022
Accepted Date: 01 November 2022

Please cite this article as: Patel, A., & Suthar, A. (2022). Analysis of urban development on land cover changes of three cities of Gujarat state, India. *Geographica Pannonica*, doi: 10.5937/gp26-39440

Analysis of urban development on land cover changes of three cities of Gujarat state, India

Alpesh M. Patel [A], Anil Suthar [B]

[A] Department of Electronics and Communication, Vishwakarma Government Engineering College, Chandkheda, Affiliated to Gujarat Technological University, Ahmedabad, Gujarat 382424, India; am_patel@gtu.edu.in. ORCID iD: https://orcid.org/0000-0001-8846-4771

[B] New L. J. Institute of Engineering and Technology, Ahmedabad, Gujarat, India; sutharac@gmail.com. ORCID iD: https://orcid.org/0000-0003-3267-8636

Received: July 31, 2022 | Revised: October 26, 2022 | Accepted: November 01, 2022

doi: 10.5937/gp26-39440

Abstract
Urbanization generally serves as a key navigator of the economic growth and development of the country. There is a need for fast and accurate urban planning to accommodate more and more people in the city area. Remote sensing technology has been used for planning the expansion and design of city areas. A novel machine learning (ML) classifier formed by combining AdaBoost and extra trees algorithm have been investigated for change detection in the urban area of three cities in the Gujarat region of India. Using Indian Remote Sensing (IRS) Resourcesat-2 LISS IV satellite images, the performance of the object-based AdaBoosted extra trees classifier (ABETC) in terms of overall accuracy (OA) and kappa coefficient (KC) for urban area change detection was compared to benchmarked object-based algorithms. As the first step in object-based classification (OBC), the Shepherd segmentation algorithm was used to segment satellite images. For all three cities, the object-based ABETC demonstrated the highest efficiency when compared to conventional classifiers. The rise in the built-up area of Ahmedabad city has been noted by 87.39 sq km from the year 2011 to 2020 showing the urban development of the city. This increase in the built-up area of Ahmedabad was compensated by the depletion of 30.26 sq. km. vegetation area, and 57.13 sq. km. of open land class. The built-up area of Vadodara and Rajkot city has been enlarged by 17.24 sq km and 6.79 sq km respectively. The highest OA of 96.04% and KC of 0.94 has been noted for a satellite image of Vadodara city with a novel object based ABETC algorithm.

Keywords: urbanization; change detection; object based classification; multispectral image

Introduction
Change detection (CD) is the cause of action for finding variation in a particular land area at different time intervals (Singh, 1989). Remote sensing technology is very useful for various applications of CD like agricultural and forest monitoring, evaluation of natural disasters, environmental and landscape tracking, and study of urban surroundings (Lu et al., 2004; Singh et al., 2011). Urbanization and its development planning play a key role in the [1]economic growth of a developing country like India. The migration of people towards city areas has generated complex problems related to traffic management, water quality, availability of fresh air, and drop in vegetation areas (Pacifici et al., 2007). Change detection

---

* Corresponding author: Alpesh M. Patel; e-mail: am_patel@gtu.edu.in

in the urban landscape is a challenging task and needs persistent monitoring due to the constant interaction of humans, deficient spectral discrimination ability, complexity of actual structures, and geometric deformation (Pacifici et al., 2009; Gamba 2012; Jia et al., 2015). The analysis of very high resolution (VHR) satellite images provides a cost-effective solution for change detection in complex urban areas. The change detection techniques are mainly bifurcated into supervised or unsupervised techniques (Coppin et al., 2002; Lu, 2004). The alteration in the atmospheric situation and radiance variation, which takes place at distinct acquisition times, are some of the exterior factors that may reduce the performance of the unsupervised method (Wang et al., 2018). The supervised CD technique is highly effective and workable compared to the unsupervised one for multitemporal satellite data (Bruzzone et al., 2000). The CD algorithms are also categorized into various categories like thresholding, image differencing, vegetation index differencing, image ratioing, transformation, and post-classification change detection. Post-classification change detection is a widely used technique for urban growth estimation (Reba et al., 2020). From the literature of the last few decades, the various post-classification change detection methods can be mainly divided into pixel based change detection (PBCD) and object based change detection (OBCD) techniques based on the basic processing unit (Zhang et al., 2018).

PBCD is a traditional approach that works on the spectral property of a single-pixel value and OBCD functions on a group of pixels having common characteristics called polygons or objects as basic processing blocks for image operations (Weih et al., 2010). PBCD techniques are largely used for medium and low-resolution satellite data, composed of finding pixel-by-pixel difference images and exploring them to acquire a change map (Zhang et al., 2018). Principal component analysis (PCA) (Deng et al., 2008) and change vector analysis (CVA) (Bruzzone et al., 2000) are some of the methods of PBCD that have been applied for the change detection task. For VHR satellite data, most PBCD techniques suffered from "salt and pepper" noise as the spatial-contextual details have not been considered (Wu et al., 2020).

OBCD methods overcome the above drawbacks by including spatial and contextual information in form of objects generated by segmenting the image into spectrally similar and meaningful polygons (Blaschke et al., 2010; Duro et al., 2012). For change detection applications in complex urban territories, object based technique has shown higher performance in form of classification accuracy (Blaschke et al., 2001). The availability of VHR satellite data and high-speed computational machines in the last few decades have assisted object based methods for change detection applications (Chen et al., 2012). For multispectral satellite data, stacking of different image bands, segmentation of the stacked image, sampling of segmented objects, extraction of various features, and classification are key operations for object based methods of classification in the post-classification change detection process. The main elements responsible for creating uncertainty during OBC operations are parameter tuning for the segmentation algorithm, strategies for selecting training data, extracting features from segments, and selection of appropriate supervised classifier and its parameters (Ma et al., 2017). The performance in terms of the accuracy of the OBCD process highly depends on the use of a proper classifier algorithm and its parameter tuning.

In recent years, different supervised classifier algorithms have been applied for object based methods of classification. Walter et al. (2004) have implemented an object based method with a supervised maximum likelihood classifier (MLC) for multispectral images. Desclée et al. (2006) introduced a statistical object based method and achieved higher overall accuracy compared to pixel based method for two different data sets. Hegazy et al. (2015) performed the change detection study of Mansoura and Talkha cities of Egypt for monitoring urban growth using a geographic information system (GIS) and found an expansion of built-up area by more than 30% and a reduction in vegetation area by 33%.

X. Wang et al. have applied the ensemble method to combine the output of multiple classifiers for object based change detection in an urban area using VHR QuickBird satellite images (Wang et al., 2018). The ensemble learning technique has shown better results in terms of classification accuracy compare to single classifiers like k-nearest neighbor (KNN), support vector machine (SVM), and random forest (RF) for the OBCD process (Wang et al., 2018). The performance of the adaptive ensemble method using extreme learning machines (ELMs) was investigated with Landsat-5 and Landsat-7 data sets and showed better results in terms of accuracy compared to single ELM for change detection (Khurana et al., 2020).

The increase in urban land area of 52.47% for Kathmandu city of Nepal was detected using Landsat-5 and Landsat-8 images for 20 years duration using remote sensing and GIS by Wang et al. (2020). This urban expansion took place with a cost of 9.28% of forest and 9.8% of agricultural land. Idowu et al. (2020) studied change detection for Lagos city of Nigeria using object based nearest neighbor classifier algorithm by integrating Landsat-7 and Sentinel 2A images. They have found 55.5% raise in the built-up area from the year 2001 to 2016 and a fall off of wetlands and forest areas.

Random forest (RF) (Stefanski et al., 2013; Wang et al., 2019; Belgiu et al., 2016) and support vector machine (SVM) (Mountrakis et al., 2011; Thanh et al., 2018; Laso et al., 2020; Pham et al., 2019) are benchmark classifiers used in object based method of classification of satellite data. Rizvi et al. (2011) have demonstrated the use of a modified cloud basis function as a kernel for artificial neural network (ANN) for QuickBird satellite images of suburban areas and found higher classification accuracy compare to radial basis function neural network (RBNN). Feng et al. (2018) have illustrated rotation forest with majority voting (RoF-MV) based OBCD method using Gaofen-2 (GF-2) satellite images of the urban area. RoF-MV method has shown a higher kappa co-efficient for accuracy measurement compared to RF-MV and ELM-MV (Feng et al., 2018). The performance in terms of the kappa co-efficient of the RF and RoF algorithm was found higher compared to SVM and Wishart classifier for Radarsat-2 satellite images and the execution time of the RF algorithm was noted very less compared to the RoF algorithm by Du et al. (2015). Colkesen et al. (2017) have compared the classification accuracy of the canonical correlation forest (CCF) algorithm with benchmarked RF and RoF algorithms and found that the CCF algorithm has higher overall accuracy for Landsat-8 (L-8) images compared to the RF algorithm but the computational time requirement for classification using CCF algorithm was also very high.

In a developing country like India, lots of people are migrating from rural to urban areas for getting better infrastructure, health, and other facilities. There is a strong need for better urban planning to accommodate migration and maintain the ecosystem. Remote sensing technology is used widely for this task. A very large amount of satellite data are available and there is a need for faster and more accurate machine learning (ML) algorithms for the analysis and investigation of urban areas for urban development planning.

The concept of the ensemble learning technique is to use several single classifiers' predictions to predict the final output for increasing the classification accuracy. For VHR satellite data, the ensemble learning methods have shown better performance in terms of classification accuracy compared to individual classifiers (Samat et al., 2018). Among the supervised classifiers, the extra trees classifier (ETC) is a highly efficient and faster ensemble classifier. It is a tree-based ensemble ML technique having different node splitting concepts by arbitrarily picking samples and cut-points (Geurts et al., 2006).

In this paper, urban area change detection of three cities of Gujarat state of India was investigated using a novel object based AdaBoosted Extra Trees Classifier for VHR satellite data. The proposed OBCD method was constructed by integrating a multi-class AdaBoost and Extra-Trees splitting algorithm with a stratified random sampling of training samples.

- The first part of the paper consists of an investigation of comparative analysis for object based DT, RF, ETC, AdaBoosted RF, and ABETC algorithms for the classification of satellite images of Ahmedabad, Vadodara, and Rajkot cities of the Gujarat region. The results have shown superior performance for ABETC in terms of classification accuracy.
- In the second part, the urban change detection investigation of the three cities has been introduced with a highly efficient object based ABETC algorithm and change detection maps for the built-up area were generated.
- A detailed change detection comparative analysis for Built-up, Vegetation, and Open land classes using object based DT, RF, ETC, ABCRF, and ABETC algorithms have been demonstrated for data sets of Ahmedabad, Vadodara, and Rajkot cities.

Study Area and Data

Gujarat has been among the highest leading industrialized states in India. Ahmedabad, Vadodara, and Rajkot are some of the major cities of the state. Ahmedabad is the largest city in terms of area as well as a major economic and industrial hub of the state. Because of urbanization, the population of the city area of Gujarat state has grown significantly in the last decades.

The satellite images from Indian Remote Sensing Satellite IRS-R2 with 5m spatial resolution have been used for the change detection study of these cities. LISS-IV (Linear Imaging Self-Scanner) sensors have been used for obtaining this very high resolution (VHR) satellite data with three (Red, Green, NIR) spectral bands. These three bands are stacked to generate the false color composites (FCC) images. The subset images of Ahmedabad with a size of 5104 × 4862 pixels for the years 2011 and 2020 are used for built-up change detection of the city. The subset images of Vadodara and Rajkot have the dimension of 3029 ×3174 pixels and 2124× 2481 pixels respectively. These subset images are covered with varying land types like vegetation, open land, and built-up. The subset of FCC images of the cities has been shown in Figure 1.

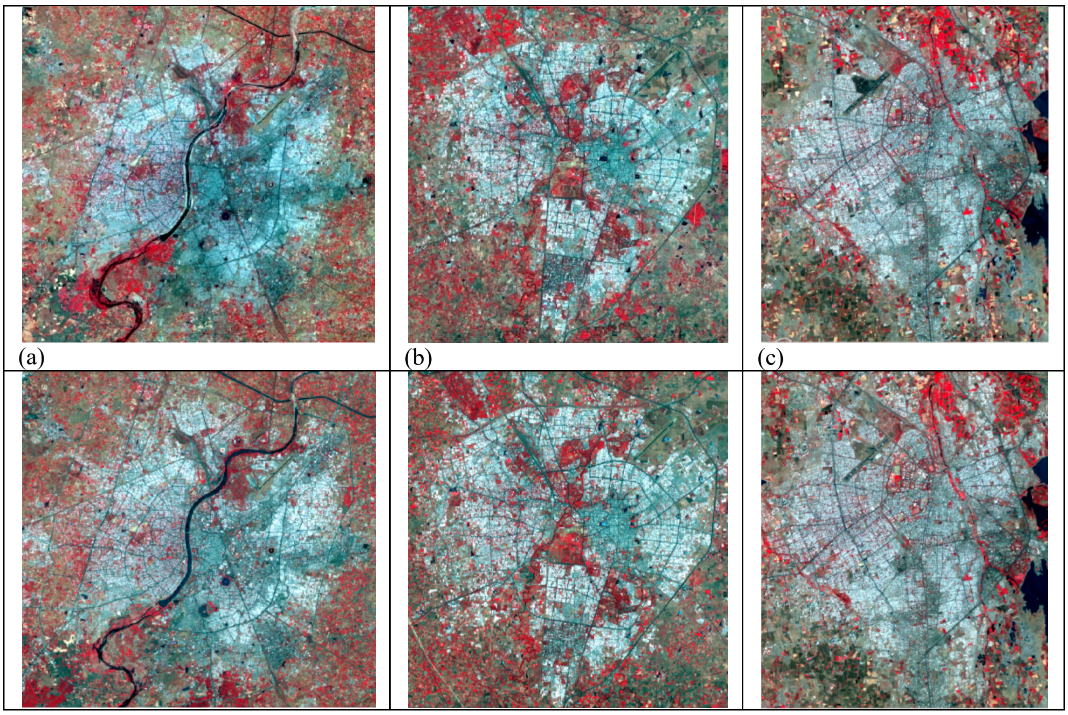

(d)	(e)	(f)

Figure 1. Images of the study area (a) Ahmedabad of year 2011, (b) Vadodara of year 2013, (c) Rajkot of year 2014, (d) Ahmedabad of year 2020, (e) Vadodara of year 2020, (f) Rajkot of year 2021

A contemporary multispectral sensor with a considerably large resolution, the resourcesat-2's LISS-IV sensor has enormous potential for creating high-quality images of land use and land cover. The brief details of the LISS-IV multispectral satellite images used in the study of change detection of the urban area are mentioned in Table 1.

Table 1. Details of the LISS-IV multispectral images

Parameter \ Sensor Instrument	LISS-IV
Spectral bands (µm)	B2: 0.52-0.59 (green), B3: 0.62-0.68 (red), B4: 0.77-0.86 (NIR)
Data quantization	10 bits
Spatial resolution (m)	5.8
Swath width	70 km in mono mode, 23 km in Multispectral mode
Detector line arrays x No of elements	1 x 12,288 Mono mode; 3 x 12,288 Multispectral mode
Revisit Period	5 days

Methodology

Change detection investigation of three cities of Gujarat using a post-classification comparison method was carried out with object based image classification having image segmentation as the most important step. The various implementation steps of the proposed method for OBCD are shown in Figure 2.

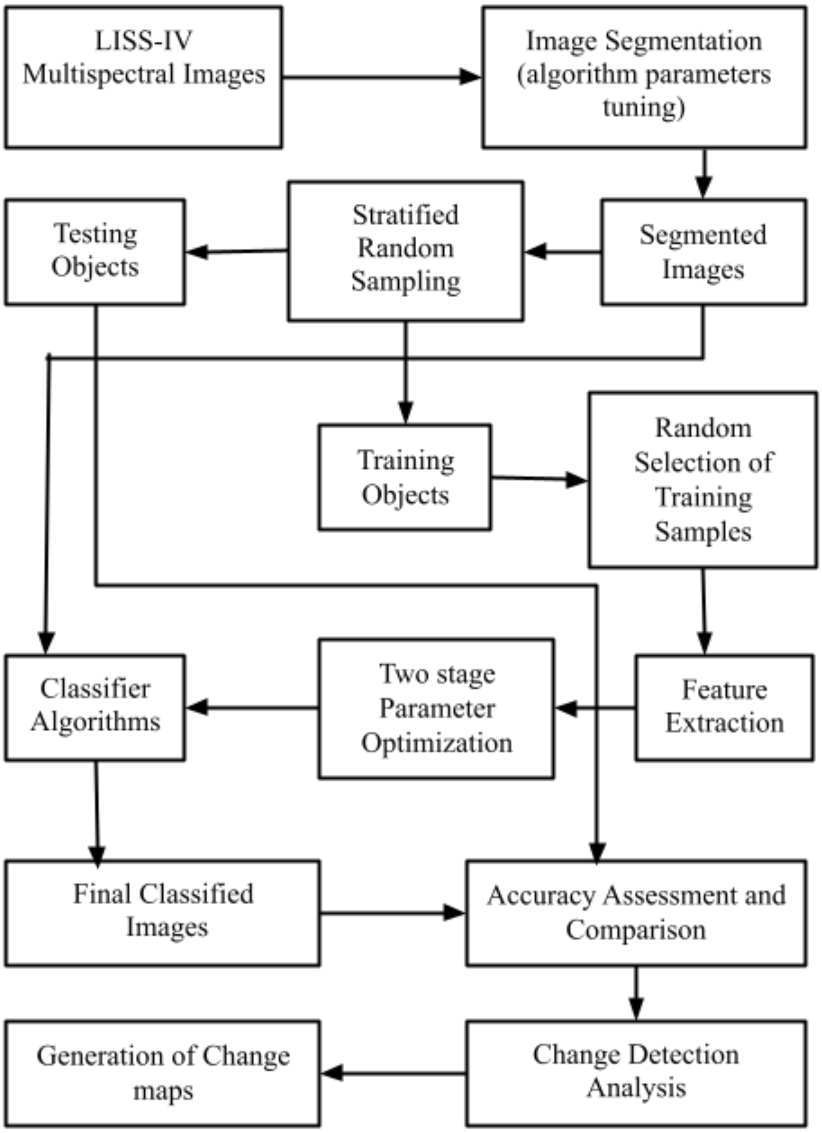

Figure 2. Flow chart of proposed OBCD method

LISS-IV multispectral images of IRS-R2 satellites for three cities are obtained. The FCC images are generated by stacking spectral bands. Image segmentation, feature extraction, object based classification and investigation of change area are the major processing steps of this OBCD method. The shepherd segmentation algorithm was used to obtain segments of these FCC images. The stratified random sampling technique was adopted for distinguishing training and testing segments. The randomly selected training samples were directed for feature extraction steps. The segments and their extracted features were utilized in the classification step with two-stage parameter optimization using the grid search cross validation (CV) module of scikit-learn (Pedregosa et al., 2011). The performance assessment of different classifier algorithms and their comparison results were summarized before picking the final classified images for change detection analysis. These classified images were used for generating change detection maps for the built-up area of three cities.

Multispectral Image Segmentation

The initial processing steps of the OBCD method consist of dividing the multispectral stacked image into spatially unbroken groups of analogous pixels with indistinguishable spectral properties known as segmentation (Blaschke et al., 2014; Singh et al., 2014). The segmentation algorithm can be of different classes like point-based, edge-based, and region-based (Schiewe et al., 2002). The aim of the segmentation process is to create segments or objects with different aspects of similarity considering various dimensions (Blaschk et al., 2010). These objects also consist of auxiliary spectral details like mean and median numbers of each band in contrast to individual pixels.

Segmentation operation was carried out using the shepherd segmentation algorithm (Shepherd et al., 2019) implemented with open source library RSGISLib (Clewley et al., 2014). The concept of segmentation is to split the image into the same kind of land cover, the complete feature, like a vegetation block, will be caught as a single object so it can be later classified into a suitable class. In the case of under segmentation, more than one feature, like vegetation and open land, may combine into a single object, and classification of such features is not feasible (Shepherd et al., 2019). As per (Shepherd et al., 2019) and (Carleer et al., 2005), a little over-segmentation can merge segments of matched class into a single object, so it was applied to maintain the performance of a later stage.

The parameters that need to be tuned for this algorithm are straightforward and less in number. Further, this algorithm is greatly scalable to large landscape areas with an iterative elimination process and is suitable for a broad range of sensors (Shepherd et al., 2019).

The shepherd algorithm operates in four different steps. In the first step, an unsupervised k-means clustering technique is applied for seeding the image. Better results were obtained with an efficient computational requirement for k-means compare to other clustering mechanisms like mean-shit, Iterative Self-Organising Data (ISOData), and fuzzy k-means (Shepherd et al., 2019). Clumping is performed as a second step in which pixels are bunched to the appropriate cluster center for making physically labeled regions. In the third step of the algorithm, the bunch below minimum dimensions are combined with spectrally nearest and bigger than itself neighbor. This iterative elimination starts with regions having the smallest size and it reduces the number of clumps drastically. Relabeling of the clump is the last step for ensuring sequential numbering of the clumps which makes the next step of classification more systematic (Shepherd et al., 2019). The two important parameters for this algorithm are the number of initial clusters k for k-means, and the minimum clump size for the elimination process (Clewley et al., 2014). The number of initial seeds k is the key parameter for making spectral differentiation among the classes. The less value of k generates few clusters which results in under-segmentation and a higher value of k creates smaller segments resulting in over segmentation. As per (Mathieu et al., 2007) and (Aguilar et al., 2013), key parameters of the shepherd segmentation algorithm were finalized using a systematic trial and error technique with a visual inspection of segmented results. The number of seed k was fixed at 60 and the maximum iteration was finalized at 100.

Shepherd et al. (2019) have investigated the performance of this segmentation algorithm in detail for three different sensors with benchmark segmentation algorithms like the multiresolution segmentation algorithm used in eCognition, the mean-shift algorithm used in Orfeo toolbox, the algorithm of Felzenszwalb and Huttenlocher, and the quick-shift algorithm and found that this algorithm compares advantageously in most resulted comparative metrics.

Labeling of Samples

Open source QGIS software (QGIS Development Team, 2019) was used to label the segments or objects generated by the segmentation process by visual exposition for all three city images. Built-up, vegetation, and open land are the three classes in which all the segments were labeled. These labeled segments were separated into training and testing segments with a stratified random sampling method. The classification performance of the classifier may be affected by the number of training segments used to train the classifier algorithm (Du et al., 2015). From each class 800 samples have been selected randomly through QGIS form which 640 samples per class were utilized for training the classifiers and 160 samples per class were used for investigating the accuracy of the classifiers.

Benchmark Classifiers

DT, RF, and SVM are the standard classifiers for object based classification of remote sensing images found in the literature. SVM technique focuses on acquiring a hyperplane for differentiating segments into fixed classes as per training data (Mountrakis et al., 2011). It is a non-parametric statistical method and advantageous where kinds of attributes are more in comparison to samples (Mountrakis et al., 2011; Pedregosa et al., 2011).

A decision tree is a type of classifier that may be described as a recursive division of the instance space and its nodes are arranged to form a rooted tree. Every internal node of the decision tree divides the instance space into a number of sub-spaces based on a specific discrete function associated with the input feature values. In the easiest and most typical scenario, each test takes into account a single attribute, dividing the instance space depending on the value of an attribute. Classification and regression trees (CART) is a non-parametric decision tree algorithm implemented for object based classification of segmented images using (Pedregosa et al., 2011). It uses Gini's impurity indicator as a splitting norm to spilt the node to form a binary tree structure. In this algorithm, the value of the target variable was estimated by using simple decision rules concluded from training data features. For a given labeled training data, this algorithm iteratively divides the feature space in such a way that the training segments with similar labels are grouped. The key parameters used for optimizing this algorithm were the number of features that need to be considered for node split and the maximum depth of the decision tree.

RF classifier is an assembly of weak learners for obtaining the best classification results and shown higher classification performance with quick operation time (Du et al., 2015). Constructing a huge number of de-correlated trees, and subsequently averaging them, is how random forests significantly modify bagging. RF algorithm has shown higher performance than tree-based ensemble techniques and bagging tree algorithms. A relatively large amount of input variables may be handled by the RF algorithm without overfitting, and they produce very good accurate predictions. RF classifier is regarded as one of the most reliable and versatile learning methods accessible. In this algorithm, trees are assembled using the re-sampling method with replacement, and the features are also randomly sampled for deciding the best node split (Du et al., 2015; Breiman et al., 2001). Finally, the majority voting method is applied for allocating class labels to unknown segments. The number of estimators, splitting criteria, amount of features, and the number specifying the depth of the tree were observed as parameters of concern for RF optimization using (Pedregosa et al., 2011).

AdaBoosted Extra Trees Classifier

In this method, extra trees classifier (ETC) and AdaBoost SAMME (Stagewise Additive Modeling using a Multi-class Exponential loss function) classifiers (Hastie et al., 2009) were combined with dual-level of its parameter optimization.

In the ETC method, the picking of cut-points for numerical attributes takes place completely randomly without considering the target variable (Geurts et al., 2006). The algorithm arbitrarily selects individual features and cut-point for each node such that completely randomized trees are generated whose formation is not dependent on the target variables of training segments (Geurts et al., 2006). Further, for developing a tree, ETC utilizes all training samples instead of bootstrap replicas used by other ensemble methods which makes it divergent from other tree-based ensemble algorithms (Samat et al., 2018).

Geurts et al. (2006) have experimentally demonstrated smaller computation time for extra trees compared to other ensemble algorithms like tree bagging and RF. This computational efficiency of ETC becomes higher as the number of features increases and is found more than ten times quicker compared to RF. This algorithm was executed using (Pedregosa et al., 2011) for object based classification of all three city images. The parameters observed as dominant parameters for optimizing the extra trees algorithm are the maximum depth of the tree, the number of trees in the forest, and the number of attributes required for node split.

The adaptive boosting algorithm presented by Freund et al. (1997) adaptively fine-tunes the errors of a weak hypothesis that is given by a weak learning algorithm for boosting the prediction of weak learners which is also called AdaBoost. For stated distribution *D* over training segments, this algorithm aims to discover the ultimate hypothesis with relatively less error. This algorithm sustains a set of weights w^t for a group of training samples *N*. These weights are normalized for evaluating distribution p^t for iteration *t* (Freund et al. 1997).

$$p^t = \frac{w^t}{\sum_{i=1}^{N} w_i^t} \tag{1}$$

This distribution applied to a weak learner that creates a hypothesis h_t with a minor error.

$$e_t = \sum_{i=1}^{N} p_i^t \; |h_t(x_i) - y_i| \tag{2}$$

The weight vector updating parameter β_t is set as

$$\beta_t = e_t/(1 - e_t) \tag{3}$$

This boosting method creates a new weight vector w^{t+1} using the new hypothesis h_t,

$$w_i^{t+1} = w_i^t \, \beta_t^{1-|h_t(x_i) - y_i|} \tag{4}$$

Succeeding *T* such iterations, the resulted hypothesis h_f integrates the results of the *T* weak hypothesis with a weighted majority vote.

The above AdaBoost algorithm was observed as an extremely successful algorithm for two-class classification issues. The AdaBoost SAMME (Stagewise Additive Modeling using a Multi-class Exponential loss function) algorithm is immensely competitive regarding misclassification error rate and is used for multi-class problems (Hastie et al., 2009). This multi-class algorithm merges the weak learners and reduces the exponential loss. This algorithm adaptively integrates a chain of weak classifiers with the weight enhancement of training segments. The weights of wrong classified samples are raised and the steps are repeated.

Parameter Optimization

The values of the parameters of ABETC were finalized in two steps. In the first step, the grid search cross validation (CV) module of (Pedregosa et al., 2011) was used for the optimization of the parameters of the ETC algorithm. The number of forest trees, maximum tree depth for expanding the nodes of trees, and a number of attributes utilized for node splitting are parameters used for optimization. The five-fold CV was used for obtaining the best values for these parameters. The optimized ETC classifier with its final parameter values was used as the base classifier in the implementation of the AdaBoost SAMME algorithm. In the second part of the parameter optimization, parameters of this combined algorithm like the learning rate, and the maximum number of weak classifiers are optimized using a fivefold CV through the grid search module. After parameter optimization, multiple ETCs were generated and trained sequentially. The weight of the training samples used for training of the above optimized base classifiers was also updated adaptively. After completing a specified number of iterations, the final prediction was produced using a majority vote. The same method was followed for implementing the AdaBoosted random forest classifier (ABRFC) and results have been compared in terms of classification accuracy.

Change detection analysis was carried out from the final classified images of object based ABETC classifier. The LISS-IV images used here have a 5m pixel resolution. So, the area represented by one pixel of the VHR image was calculated as 25 square meters. Then the number of pixels of each class and their area in square kilometers were calculated for images of three cities on different dates. In the last step change map for the built-up area of three cities was generated using (Clewley et al., 2014).

Experimental Results and Discussion

The LISS-IV images of Ahmedabad for the years 2011 and 2020 have been classified using an object based method with the shepherd segmentation algorithm. Tables 2 and 3 show the performance comparison of DT, RF, ETC, ABRFC, and ABETC classifiers for these images. The overall accuracy (OA) and kappa coefficient (KC) are measured and considered as evaluation criteria for the above classification algorithms. All the segments of the images have been labeled in three different classes called vegetation, built-up and open land. 160 samples from each class have been used for testing the performance of the classifiers and 640 samples from each class were used to train the classifiers. The selection process of training and testing segments was done with a stratified random sampling technique through QGIS software.

Table 2. Accuracy Statistics comparison for DT, RF, ETC, ABRFC, and ABETC Classifiers for Ahmedabad 2020 dataset

Classes	DT		RF		ETC		ABCRF		ABETC	
	UA	PA	UA	PA	UA	PA	UA	PA	UA	PA
Vegetation	0.93	0.93	0.93	0.94	0.93	0.94	0.94	0.94	0.93	0.95
Open land	0.94	0.94	0.96	0.95	0.98	0.95	0.98	0.95	0.98	0.97
Built-up	0.78	0.77	0.82	0.83	0.80	0.85	0.80	0.85	0.84	0.85
OA	89.56		91.48		92.08		92.03		93.46	
KC	0.86		0.89		0.89		0.89		0.91	

Table 3. Accuracy Statistics comparison for DT, RF, ETC, ABRFC, and ABETC Classifiers for Ahmedabad 2011 dataset

Classes	DT		RF		ETC		ABCRF		ABETC	
	UA	PA	UA	PA	UA	PA	UA	PA	UA	PA
Vegetation	0.87	0.95	0.87	0.96	0.87	0.96	0.88	0.96	0.86	0.96
Open land	0.95	0.92	0.98	0.95	0.98	0.95	0.98	0.96	0.98	0.95
Built-up	0.82	0.84	0.84	0.85	0.85	0.87	0.85	0.86	0.87	0.88
OA	89.55		92.08		92.61		92.58		93.05	
KC	0.87		0.90		0.90		0.90		0.91	

Table 4. Accuracy Statistics comparison for DT, RF, ETC, ABRFC, and ABETC Classifiers for Vadodara 2020 dataset

Classes	DT		RF		ETC		ABCRF		ABETC	
	UA	PA	UA	PA	UA	PA	UA	PA	UA	PA
Vegetation	0.97	0.95	0.95	0.97	0.96	0.96	0.96	0.96	0.96	0.97
Open land	0.93	0.90	0.93	0.94	0.94	0.95	0.94	0.95	0.96	0.95
Built-up	0.85	0.92	0.94	0.92	0.94	0.93	0.95	0.92	0.95	0.96
OA	91.90		94.04		94.80		94.51		96.04	
KC	0.88		0.91		0.92		0.92		0.94	

Table 5. Accuracy Statistics comparison for DT, RF, ETC, ABRFC, and ABETC Classifiers for Rajkot 2021 dataset

Classes	DT		RF		ETC		ABCRF		ABETC	
	UA	PA	UA	PA	UA	PA	UA	PA	UA	PA
Vegetation	0.96	0.91	0.98	0.94	0.98	0.95	0.98	0.96	0.97	0.95
Open land	0.93	0.90	0.90	0.96	0.92	0.95	0.97	0.92	0.96	0.95
Built-up	0.83	0.92	0.94	0.88	0.91	0.90	0.89	0.98	0.93	0.97
OA	90.93		93.22		93.55		94.93		95.53	
KC	0.86		0.90		0.90		0.92		0.93	

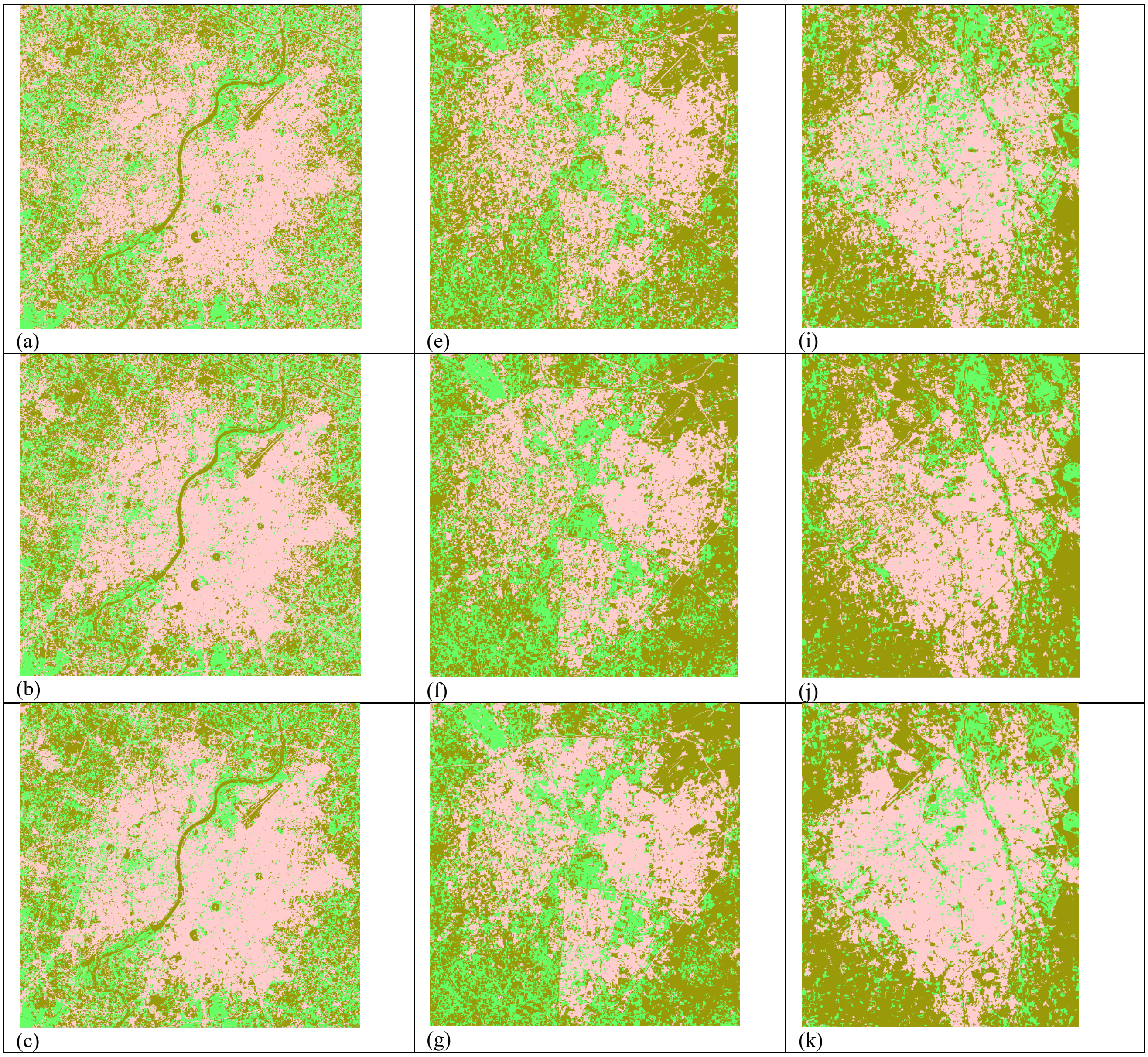

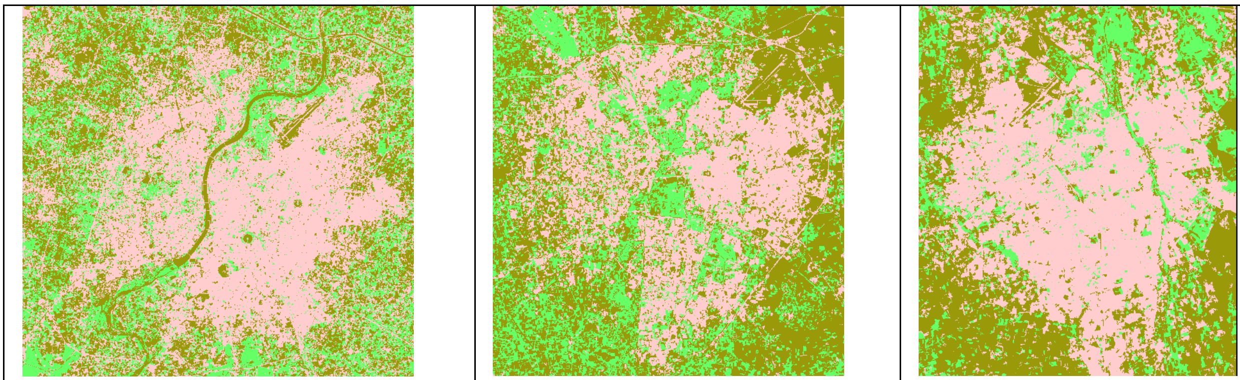

(d) (h) (l)

Vegetation Built-up Open lar

Figure 3. classified images of (a) DT, (b) RF, (c) ETC and (d) ABRFC classifiers for Ahmedabad 2020 data set; (e) DT, (f) RF, (g) ETC and (h) ABRFC classifiers for Vadodara 2020 data set and (i) DT, (j) RF, (k) ETC and (l) ABRFC classifiers for Rajkot 2021 data set

The class-wise performance evaluation in terms of user's accuracy (UA), and producer's accuracy (PA) is also mentioned in the accuracy statistic tables. The built-up area change is the key parameter for demonstrating the urban development of any city. Another concern class is the vegetation area for maintaining a good ecosystem in growing cities. Among the DT, RF, and ETC classifiers, OA and KC of the ETC algorithm were found higher as shown in Tables 2 and 3 for Ahmedabad data sets. The consolidated AdaBoosted Extra Trees Classifier (ABETC) has shown the highest performance with OA of 93.46% and KC of 0.91 for the Ahmedabad data set for the year 2020. For Ahmedabad 2011 dataset also, the object based ABETC algorithm has excelled with an OA of 93.05 % among these five algorithms. The classification accuracy in terms of overall accuracy was found better for the ABRFC algorithm compare to the RF algorithm.

The performance comparison of these object based classification algorithms for the Vadodara dataset of the year 2020 and the Rajkot dataset of the year 2021 is mentioned in Tables 4 and 5. For these datasets also, the ETC algorithm has shown higher OA compared to DT and RF. The ETC has indicated overall accuracy of 94.8% and 93.55% for Vadodara 2020 and Rajkot 2021 images respectively.

Compare to ABRFC, the ABETC has shown superior results in terms of OA and KC for both these images. The highest value of the kappa coefficient was 0.94 with an object based ABETC classifier for Vadodara 2020 data set. As shown in Tables 4 and 5, the integrated ABETC algorithm has demonstrated superior performance among these five object based algorithms with an OA of 96.04% for the Vadodara 2021 image and 95.53% for the Rajkot 2021image.

Chen et al. (2017) used a multiple classifier system (MCS) to assess a time series of cloud-free Landsat-5 TM, Landsat-7 enhanced thematic mapper plus (ETM+), and Landsat-8 operational land imager (OLI) sensors to map LUC changes in Guangzhou, the capital city of Guangdong province in China, from 1987 to 2015. SVM, C4.5 decision trees, and artificial neural networks (ANN) were employed as the training algorithms of the base classifiers for the novel MCS classification approach, which resulted in a higher Kappa coefficient (0.87) than any base classifier. The best overall accuracy was attained by MCS based on Weight Vector enhanced by AdaBoost, which scored 88.12%. SVM, ANN, and C4.5 came in second, third, and fourth, respectively, with 82.85%, 81.77%, and 80.20% overall accuracy.

To obtain results with a better degree of accuracy, Avashia et al. (2020) used numerous categorization techniques. Using Landsat images, they investigated the evaluation of various classification algorithms, including hybrid, unsupervised, decision tree categorization, and object-based image analysis (OBIA), for mapping out the changes in land usage in Indian cities. The findings imply that employing multi-level classification for various Indian cities at various stages of the classification process will increase accuracy levels. They employed DTC and OBIA classification methods for difficult classes. For Ahmedabad, Vadodara, and Rajkot cities, the highest overall accuracy obtained by them are 90.06%, 91.93%, and 89.94% respectively. The best kappa co-efficient value recorded by them for Ahmedabad, Vadodara, and Rajkot city is 0.88, 90.04, and 87.87 respectively.

The final classified images of the Ahmedabad 2020 data set, Vadodara 2020 data set, and Rajkot 2021 dataset using object based DT, RF, ETC, and ABRFC classifiers are shown in Figure 3. All the images have been classified into vegetation, open land, and built-up class. The vegetation class was shown in green color and the built-up class in dark off-white color. As mentioned in Tables 2 - 5, the object based ABETC classifier has indicated the best performance with regard to OA and KC, the object based change detection (OBCD) analysis was carried out using classified images of this classifier.

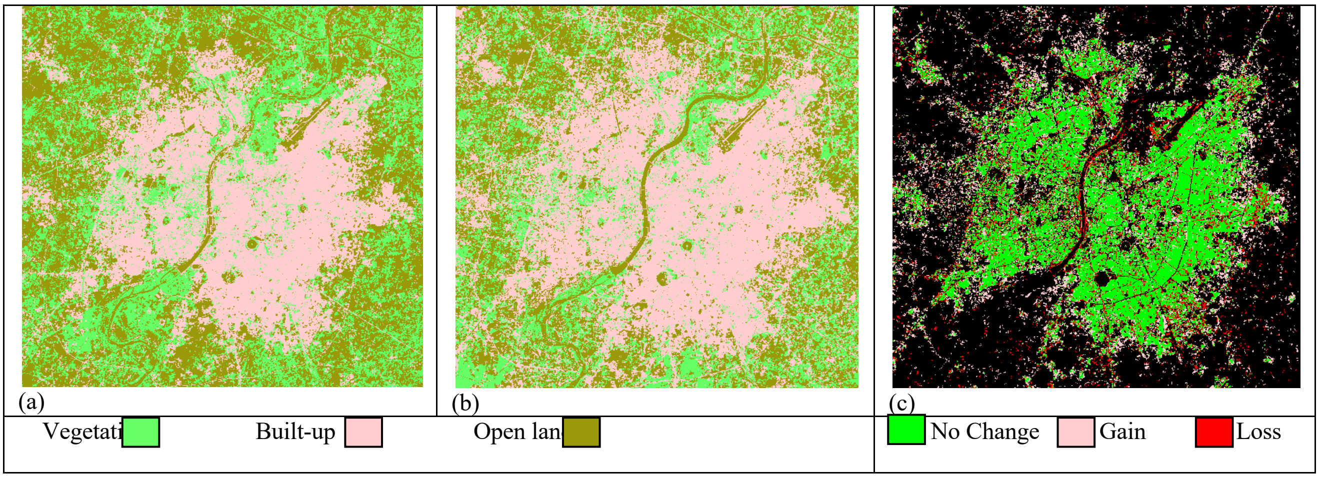

Figure 4. OBCD results using ABETC for Ahmedabad Data set. (a) Classified Image of the year 2011 (b) Classified Image of the year 2020 (c) Built-up area change map of Ahmedabad

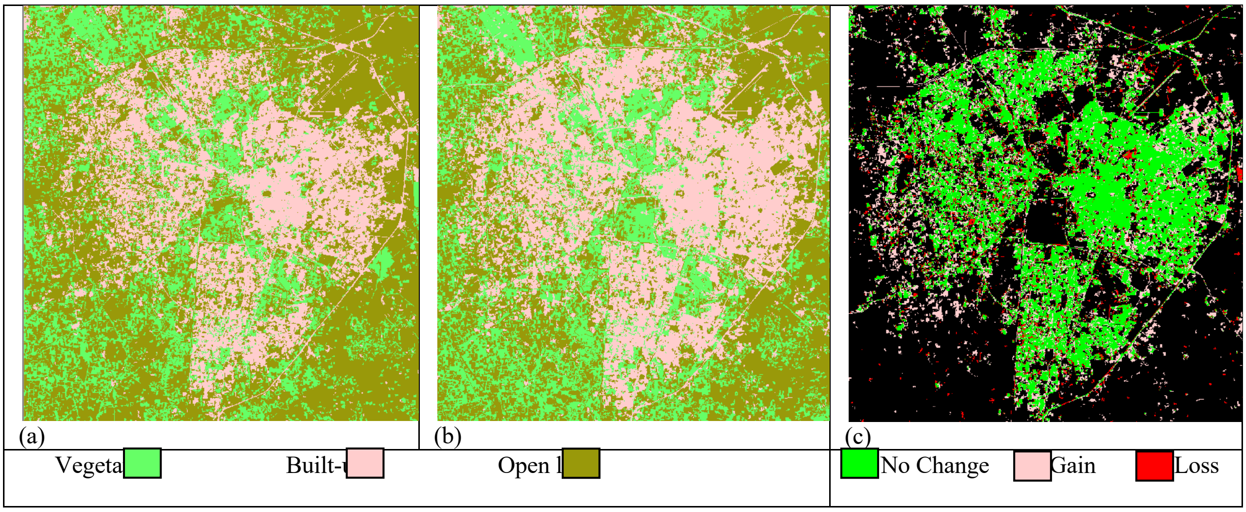

Figure 5. OBCD results using ABETC for Vadodara Data set. (a) Classified Image of the year 2013 (b) Classified Image of the year 2020 (c) Built-up area change map of Vadodara

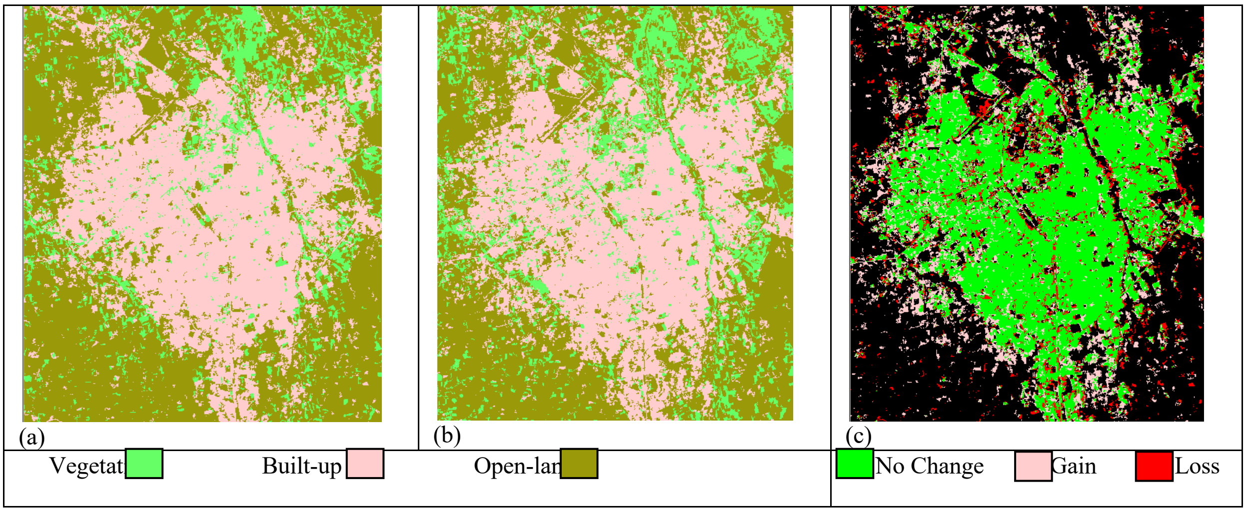

Figure 6. OBCD results using ABETC for Rajkot Data set. (a) Classified Image of the year 2014 (b) Classified Image of the year 2021 (c) Built-up area change map of Rajkot

Figure 4 shows the result of the OBCD map of a built-up class of Ahmedabad data set from the year 2011 to 2020. The classified images of the year 2011 and 2020 using the ABETC classifier are displayed in Figure 4(a) and Figure 4(b) respectively. A remarkable increase in built-up area from the year 2011 to 2020 can be visualized from these images. Using these classified images, a change detection map was generated as shown in Figure 4(c). In this map, the green color indicates that this area was part of the built-up class in the years 2011 and 2020. Because of urban development, some of the open land and vegetation area has been converted into built-up areas. This conversion was shown as a gain in a built-up area with a dark off white color. Similarly, change from built-up to vegetation or open land class was indicated with red color in the change detection map. The classified results of the ABETC classifier of Vadodara 2020 and Rajkot 2021 datasets are shown in Figure 5 and Figure 6. The significant rise in built-up class can be noticed from the year 2013 (Figure 5(a)) to 2020 (Figure 5(b)) classified images of Vadodara. Figure 5(c) shows the OBCD map of the Vadodara data set, produced using classified images of the ABETC classifier. From Figure 5(c), the gain in the built-up class can be found in the outer part of the city area. The change detection map of the Rajkot data set, fabricated using object based ABETC classified results (Figure 6(a) and Figure 6(b)) is shown in Figure 6(c). The major increase in built-up class can be visualized, as illustrated in Figure 6(c), along three sides of the city area.

Table 6. Change detection Statistics for Ahmedabad data set

Classes	Year 2011		Year 2020		Overall Change	
	Area sq. km.	% Area	Area sq. km.	% Area	Area sq. km.	% Change
Built-up	214.40	34.67	301.79	48.80	87.39	40.76
Vegetation	159.52	25.79	129.26	20.90	-30.26	-18.97
Open land	244.52	39.54	187.39	30.30	-57.13	-23.36
Total	618.44	100.00	618.44	100.00		

Table 7. Change detection Statistics for Vadodara data set

Classes	Year 2013		Year 2020		Overall Change	
	Area sq. km.	% Area	Area sq. km.	% Area	Area sq. km.	% Change
Built-up	63.26	26.32	80.50	33.49	17.24	27.25
Vegetation	52.72	21.93	61.16	25.45	8.44	16.01
Open land	124.37	51.75	98.69	41.06	-25.68	-20.65
Total	240.35	100.00	240.35	100.00		

Table 8. Change detection Statistics for Rajkot data set

Classes	Year 2014		Year 2021		Overall Change	
	Area sq. km.	% Area	Area sq. km.	% Area	Area sq. km.	% Change
Built-up	50.42	38.27	57.21	43.43	6.79	13.47
Vegetation	13.53	10.27	19.05	14.46	5.52	40.80
Open land	67.79	51.46	55.48	42.11	-12.31	-18.16
Total	131.74	100.00	131.74	100.00		

The change detection statistics of the Ahmedabad, Vadodara, and Rajkot data set are shown in Table 6, 7, and 8 respectively. The built-up area of Ahmedabad was changed from 214.4 sq. km. in the year 2011 to 301.79 sq. km. in the year 2020. This increase in built-up class was compensated by the depletion of 30.26 sq. km. vegetation area and 57.13 sq. km. of open land class. From the year 2011 to 2020, the built-up area of Ahmedabad has increased by 40.76% which shows the very high rate of urban development and migration of people in the city area. The 18.97% loss in vegetation class is also a matter of concern for maintaining the ecosystem of the city. As shown in Table 7, the built-up area increased by 17.24 sq. km from the year 2013 to the year 2020 for Vadodara city. The vegetation class was also expanded by 8.44 sq. km. and the open land area shrunk by 25.68 sq. km. The built-up class of Rajkot for the year 2014 was 50.42 sq. km. and it has increased to 57.21 sq. km. in the year 2021. The growth in the built-up and vegetation class of Rajkot was adjusted to 12.31 sq. km. of open land area. The area statistic graph of this analysis is shown in Figure 7. The expansion of the built-up area and decline in the vegetation and open area can be visualized from this graph.

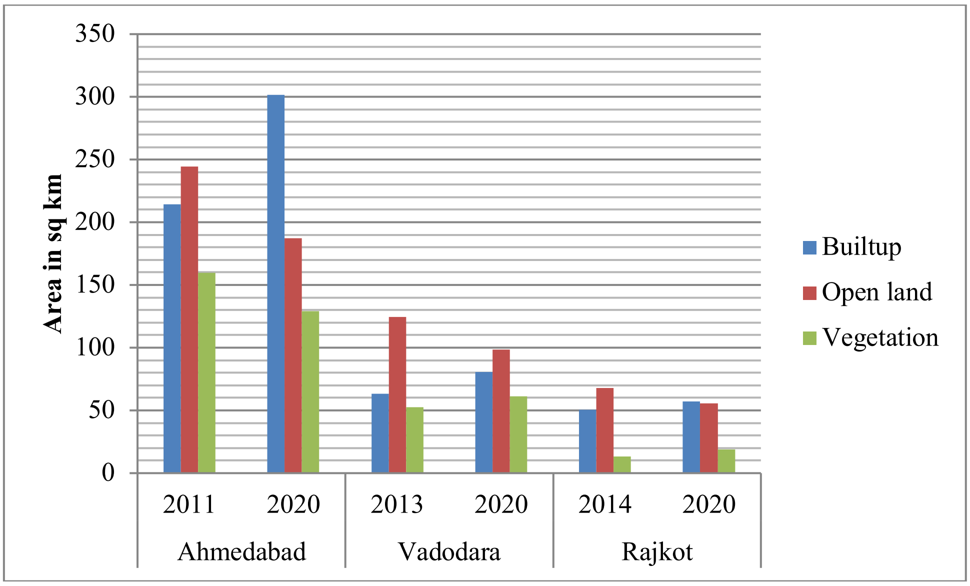

Figure 7. Area statistic graph of three data sets

Table 9. Change detection comparison for Ahmedabad data set (Area in sq. km.)

Classes	DT		RF		ETC		ABCRF		ABETC	
	2011	2020	2011	2020	2011	2020	2011	2020	2011	2020
Built-up	205.91	308.64	225.4	295.47	214.96	294.09	223.68	313.81	214.4	301.79
Vegetation	144.21	124.3	155.35	132.67	161.64	137.16	154.6	126.42	159.52	129.26
Open land	268.32	185.5	237.69	190.3	241.84	187.19	240.16	178.21	244.52	187.39
Total	618.44	618.44	618.44	618.44	618.44	618.44	618.44	618.44	618.44	618.44

Table 10. Change detection comparison for Vadodara data set (Area in sq. km.)

Classes	DT		RF		ETC		ABCRF		ABETC	
	2011	2020	2011	2020	2011	2020	2011	2020	2011	2020
Built-up	68.67	82.9	65.23	81.95	63.85	81.37	62.58	80.96	63.26	80.5
Vegetation	45.1	56.94	53.41	57.15	53.99	60.7	51.14	57.13	52.72	61.16
Open land	126.58	100.51	121.71	101.25	122.5	98.29	126.63	102.26	124.37	98.69
Total	240.35	240.35	240.35	240.35	240.34	240.36	240.35	240.35	240.35	240.35

Table 11. Change detection comparison for Rajkot data set (Area in sq. km.)

Classes	DT		RF		ETC		ABCRF		ABETC	
	2011	2020	2011	2020	2011	2020	2011	2020	2011	2020
Built-up	50.79	54.13	51.17	53.97	51.38	56.94	50.71	56.47	50.42	57.21
Vegetation	12.37	18.93	13.22	18.85	13.28	19.67	13.02	19.65	13.53	19.05
Open land	68.58	58.68	67.35	58.91	67.08	55.13	68.01	55.62	67.79	55.48
Total	131.74	131.74	131.74	131.73	131.74	131.74	131.74	131.74	131.74	131.74

The change detection comparisons of the Ahmedabad, Vadodara, and Rajkot data sets are shown in Tables 9, 10, and 11 respectively. These tables show the area obtained for Built-up, Vegetation, and Open land classes using object based DT, RF, ETC, ABCRF, and ABETC algorithms. The change detection comparison graphs of the Ahmedabad, Vadodara, and Rajkot cities using these algorithms are revealed in Figure 8, Figure 9, and Figure 10 respectively. The enlargement of the built-up class and decrease in the open land class can be visualized for all these algorithms from these graphs.

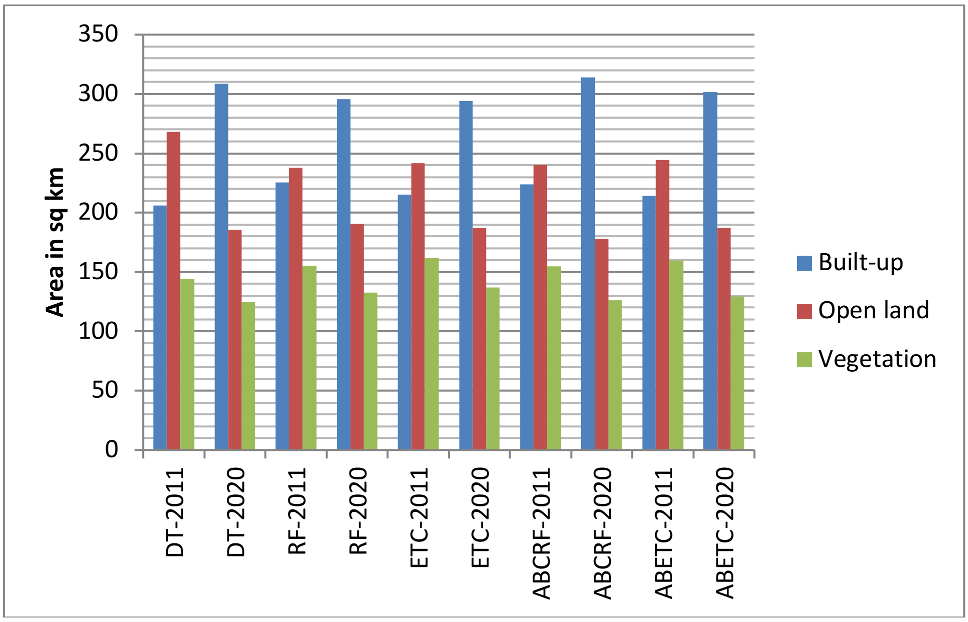

Figure 8. Area comparison graph of Ahmedabad data sets

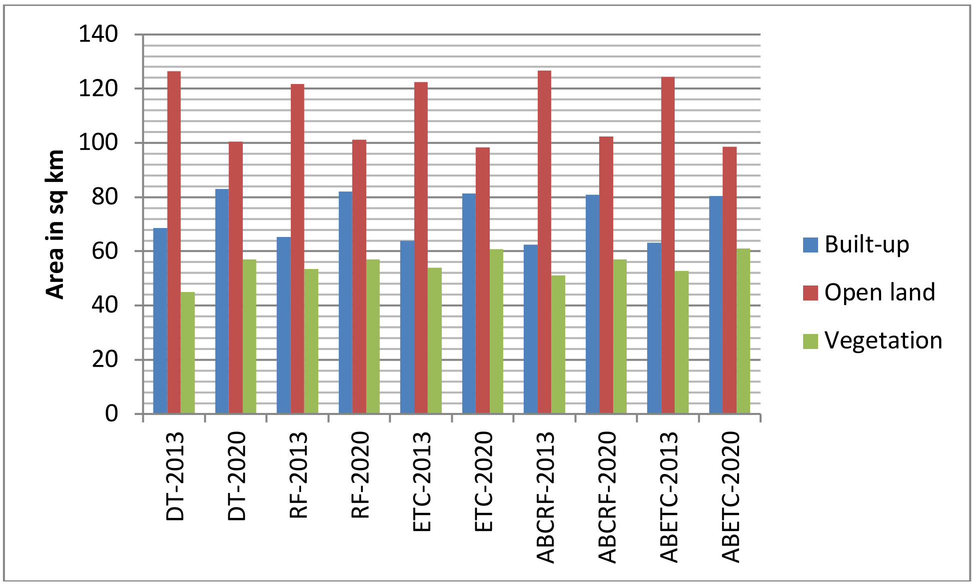

Figure 9. Area comparison graph of Vadodara data sets

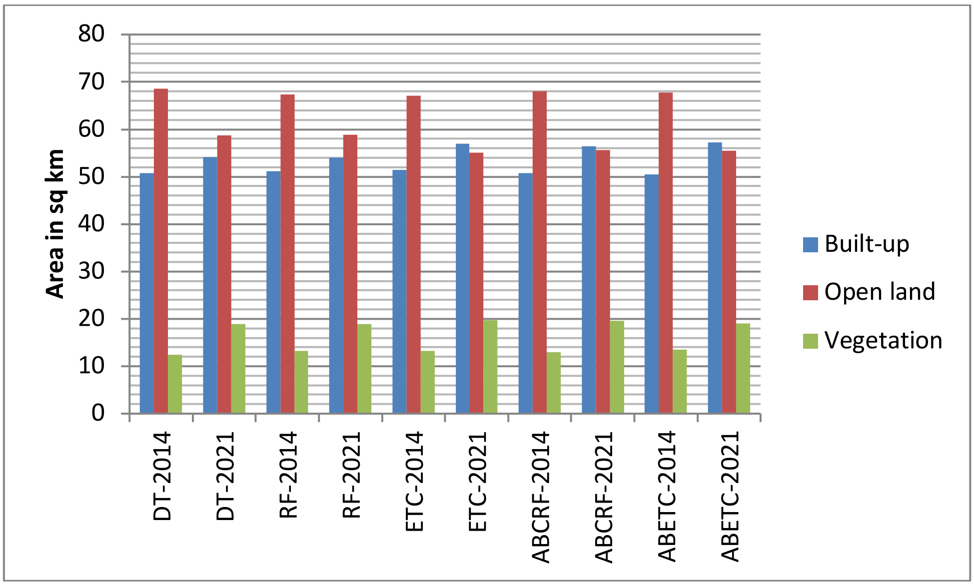

Figure 10. Area comparison graph of Rajkot data sets

Tables 2 to 5 have mentioned the various accuracy statistics and comparison of five object based classifier algorithms for the Ahmedabad, Vadodara, and Rajkot data sets. The object based integrated AdaBoosted extra trees classifier (ABETC) has demonstrated the highest performance in terms of OA and KC for all the data sets. The results of this highly efficient classifier were used for change detection analysis (Table 6-8) and change map generation. The rise in a built-up area for Ahmedabad was found higher compared to the Vadodara and Rajkot data set with a significant fall off of vegetation class.

Conclusion

In the past few years, the migration of people from rural to urban areas has increased in the fast-developing state of Gujarat. So, speedy and perfect planning of infrastructure development and its implementation considering the upcoming future environmental issues is very necessary. In this paper, a novel OBCD technique is presented by consolidating the multi-class AdaBoost SAMME algorithm and the extra trees ensemble method with the Shepherd algorithm as a segmentation step. The accuracy statistics of object based ABETC classifiers were compared with object based DT, RF, ETC, and ABRFC by measuring OA and KC. This comparative analysis was carried out with Ahmedabad, Vadodara, and Rajkot data sets. The object based ABETC has illustrated the most accurate results concerning classification accuracy with a kappa coefficient of 0.94 for the Vadodara data set. The change detection statistics and built-up change map were generated from classified images of object based ABETC classifiers. A rise of 40.76% in the built-up area has been noted from the year 2011 to 2020 for Ahmedabad with a remarkable decline in vegetation area. In the last seven years, a 27.25% increase in the built-up area of Vadodara and 13.47% growth in the built-up class of Rajkot have been measured. The expansion of the built-up class shows the growth of urbanization in the city area. For future investigation of micro details of the urban area, ultra high resolution images with more bands and focused on some specific part of the city may be used.

Funding
This research received no specific grant from any funding agency in the public, commercial, or not-for-profit sectors.

Declaration
Conflict of interest: The authors declare that they have no conflict of interest.

Acknowledgment
We gratefully acknowledge the Space Applications Centre of the Indian Space Research Organisation, Ahmedabad, India for providing IRS LISS-IV multispectral Images.

References

Aguilar, M. A., Saldaña, M. M., & Aguilar, F. J. (2013). GeoEye-1 and WorldView-2 pan-sharpened imagery for object-based classification in urban environments. *International Journal of Remote Sensing 34*(7), 2583-2606. https://doi.org/10.1080/01431161.2012.747018

Avashia, V., Parihar, S., & Garg, A. (2020). Evaluation of classification techniques for land use change mapping of Indian cities. *Journal of the Indian Society of Remote Sensing*, *48*(6), 877-908.

Belgiu, M., & Drăguţ, L. (2016). Random forest in remote sensing: A review of applications and future directions. *ISPRS journal of photogrammetry and remote sensing 114*, 24-31. https://doi.org/10.1016/j.isprsjprs.2016.01.011

Blaschke, T. (2010). Object based image analysis for remote sensing. *ISPRS Journal of Photogrammetry and Remote Sensing 65*(1), 2–16. https://doi.org/10.1016/j.isprsjprs.2009.06.004

Blaschke, T., & J. Strobl, J. (2001). Whats wrong with pixels? Some recent developments interfacing remote sensing and GIS. *GeoBIT/GIS 6*(1), 12–17.

Blaschke, T., Hay, G. J., Kelly, M., Lang, S., Hofmann, P., Addink, E., Feitosa, R.Q., Van der Meer, F., Van der Werff, H., Van Coillie, F., & Tiede, D. (2014). Geographic object-based image analysis–towards a new paradigm. *ISPRS journal of photogrammetry and remote sensing 87*, 180-191. https://doi.org/10.1016/j.isprsjprs.2013.09.014

Breiman, L. (2001). Random forests. *Machine learning 45*(1), 5-32.

Bruzzone, L., & Prieto, D. F. (2000). Automatic analysis of the difference image for unsupervised change detection. *IEEE Transactions on Geoscience and Remote sensing 38*(3), 1171-1182. DOI: 10.1109/36.843009

Bruzzone, L., & Prieto, D. F. (2000). Automatic analysis of the difference image for unsupervised change detection. *IEEE Transactions on Geoscience and Remote sensing 38*(3), 1171-1182. DOI: 10.1109/36.843009

Carleer, A. P., Debeir, O., & Wolff, E. (2005). Assessment of very high spatial resolution satellite image segmentations. *Photogrammetric Engineering & Remote Sensing 71*(11), 1285-1294. https://doi.org/10.14358/PERS.71.11.1285

Chen, G., Hay, G. J., Carvalho, L. M., & Wulder, M. A. (2012). Object-based change detection. *International Journal of Remote Sensing 33*(14), 4434-4457. https://doi.org/10.1080/01431161.2011.648285

Chen, Y., Dou, P., & Yang, X. (2017). Improving land use/cover classification with a multiple classifier system using AdaBoost integration technique. Remote Sensing *9*(10), 1055.

Clewley, D., Bunting, P., Shepherd, J., Gillingham, S., Flood, N., Dymond, J., Lucas, R., Armston, J., & Moghaddam, M. (2014). A python-based open source system for geographic object-based image analysis (GEOBIA) utilizing raster attribute tables. *Remote Sensing 6*(7), 6111-6135. DOI:10.3390/rs6076111

Colkesen, I., & Kavzoglu, T. (2017). Ensemble-based canonical correlation forest (CCF) for land use and land cover classification using sentinel-2 and Landsat OLI imagery. *Remote Sensing Letters 8*(11), 1082–1091. https://doi.org/10.1080/2150704X.2017.1354262

Coppin, P., Lambin, E., Jonckheere, I., & Muys, B. (2002). Digital change detection methods in natural ecosystem monitoring: A review. *Analysis of multi-temporal remote sensing images*, 3-36. https://doi.org/10.1142/9789812777249_0001

Deng, J. S., Wang, K., Deng, Y. H., & Qi, G. J. (2008). PCA based land use change detection and analysis using multitemporal and multisensor satellite data. *International Journal of Remote Sensing 29*(16), 4823-4838. https://doi.org/10.1080/01431160801950162

Desclée, B., Bogaert, P., & Defourny, P. (2006). Forest change detection by statistical object-based method. *Remote sensing of environment 102*(1-2), 1-11. DOI:10.1016/j.rse.2006.01.013

Du, P., Samat, A., Waske, B., Liu, S., & Li, Z. (2015). Random Forest and Rotation Forest for fully polarized SAR image classification using polarimetric and spatial features. *ISPRS Journal of Photogrammetry and Remote Sensing 105*, 38–53. https://doi.org/10.1016/j.isprsjprs.2015.03.002

Duro, D. C., Franklin, S. E., & Dubé, M. G. (2012). A comparison of pixel-based and object-based image analysis with selected machine learning algorithms for the classification of agricultural landscapes using SPOT-5 HRG imagery. *Remote Sensing of Environment 118*, 259–272. https://doi.org/10.1016/j.rse.2011.11.020

Feng, W., Sui, H., Tu, J., Huang, W., Xu, C., & Sun, K. (2018). A novel change detection approach for multi-temporal high-resolution remote sensing images based on rotation forest and coarse-to-fine uncertainty analyses. *Remote Sensing 10*(7). https://doi.org/10.3390/rs10071015

Freund, Y., & Schapire, R. E. (1997). A decision-theoretic generalization of on-line learning and an application to boosting. *Journal of computer and system sciences 55*(1), 119-139. https://doi.org/10.1006/jcss.1997.1504

Gamba, P. (2012). Human settlements: A global challenge for EO data processing and interpretation. *Proceedings of the IEEE 101*(3), 570-581. DOI:10.1109/JPROC.2012.2189089

Geurts, P., Ernst, D., & Wehenkel, L. (2006). Extremely randomized trees. *Machine Learning 63*(1), 3–42. https://doi.org/10.1007/s10994-006-6226-1

Hastie, T., Rosset, S., Zhu, J., & Zou, H. (2009). Multi-class adaboost. *Statistics and its Interface 2*(3), 349-360. DOI: https://dx.doi.org/10.4310/SII.2009.v2.n3.a8

Hegazy, I. R., & Kaloop, M. R. (2015). Monitoring urban growth and land use change detection with GIS and remote sensing techniques in Daqahlia governorate Egypt. *International Journal of Sustainable Built Environment 4*(1), 117–124. https://doi.org/10.1016/j.ijsbe.2015.02.005

Idowu, T. E., Waswa, R. M., Lasisi, K., Nyadawa, M., & Okumu, V. (2020). Object-based multi-temporal land use land cover change detection of the coastal city of Lagos, Nigeria using post-classification comparison technique. *South African Journal of Geomatics 9*(2), 136–148. DOI:10.4314/sajg.v9i2.11

Jia, S., Zhang, X., & Li, Q. (2015). Spectral–Spatial Hyperspectral Image Classification Using l1/2 Regularized Low-Rank Representation and Sparse Representation-Based Graph Cuts. *IEEE Journal of Selected Topics in Applied Earth Observations and Remote Sensing 8*(6), 2473-2484. DOI: 10.1109/JSTARS.2015.2423278

Khurana, M., & Saxena, V. (2020). A Unified Approach to Change Detection Using an Adaptive Ensemble of Extreme Learning Machines. *IEEE Geoscience and Remote Sensing Letters 17*(5), 794–798. https://doi.org/10.1109/LGRS.2019.2933906

Laso, F. J., Benítez, F. L., Rivas-Torres, G., Sampedro, C., & Arce-Nazario, J. (2020). Land cover classification of complex agroecosystems in the non-protected highlands of the Galapagos Islands. *Remote sensing 12*(1), 65. https://doi.org/10.3390/rs12010065

Lu, D., Mausel, P., Brondizio, E., & Moran, E. (2004). Change detection techniques. *International journal of remote sensing 25*(12), 2365-2401. https://doi.org/10.1080/0143116031000139863

Lu, D., Mausel, P., Brondizio, E., & Moran, E. (2004). Change detection techniques. *International journal of remote sensing 25*(12), 2365-2401. https://doi.org/10.1080/0143116031000139863

Ma, L., Li, M., Ma, X., Cheng, L., Du, P., & Liu, Y. (2017). A review of supervised object-based land-cover image classification. *ISPRS Journal of Photogrammetry and Remote Sensing 130*, 277–293. https://doi.org/10.1016/j.isprsjprs.2017.06.001

Mathieu, R., Aryal, J., & Chong, A. K. (2007). Object-based classification of Ikonos imagery for mapping large-scale vegetation communities in urban areas. *Sensors 7*(11), 2860-2880. https://doi.org/10.3390/s7112860

Mountrakis, G., Im, J., & Ogole, C. (2011). Support vector machines in remote sensing: A review. *ISPRS Journal of Photogrammetry and Remote Sensing 66*(3), 247-259. https://doi.org/10.1016/j.isprsjprs.2010.11.001

Pacifici, F., Chini, M., & Emery, W. J. (2009). A neural network approach using multi-scale textural metrics from very high-resolution panchromatic imagery for urban land-use classification. *Remote Sensing of Environment 113*(6), 1276-1292. DOI:10.1016/J.RSE.2009.02.014

Pacifici, F., Del Frate, F., Solimini, C., & Emery, W. J. (2007). An innovative neural-net method to detect temporal changes in high-resolution optical satellite imagery. *IEEE Transactions on Geoscience and Remote Sensing 45*(9), 2940-2952. DOI:10.1109/TGRS.2007.902824

Pedregosa, F., Varoquaux, G., Gramfort, A., Michel, V., Thirion, B., Grisel, O., Blondel, M., Prettenhofer, P., Weiss, R., Dubourg, V., & Duchesnay, E. (2011). Scikit-learn: Machine learning in Python. *Journal of machine Learning research 12*, 2825-2830.

Pham, V. M., Van Nghiem, S., Bui, Q. T., Pham, T. M., & Van Pham, C. (2019). Quantitative assessment of urbanization and impacts in the complex of Huế Monuments, Vietnam. *Applied Geography 112*, 102096. https://doi.org/10.1016/j.apgeog.2019.102096

QGIS Development Team. (2019). QGIS (Version 2.18). Open Source Geospatial Foundation Project. https://qgis.org/en/site/.

Reba, M., & Seto, K. C. (2020). A systematic review and assessment of algorithms to detect, characterize, and monitor urban land change. *Remote Sensing of Environment 242*, 111739. https://doi.org/10.1016/j.rse.2020.111739

Rizvi, I. A., & Mohan, B. K. (2011). Object-based image analysis of high-resolution satellite images using modified cloud basis function neural network and probabilistic relaxation labeling process. *IEEE Transactions on Geoscience and Remote Sensing 49*(12), 4815-4820. DOI: 10.1109/TGRS.2011.2171695

Samat, A., Persello, C., Liu, S., Li, E., Miao, Z., & Abuduwaili, J. (2018). Classification of VHR Multispectral Images Using ExtraTrees and Maximally Stable Extremal Region-Guided Morphological Profile. *IEEE Journal of Selected Topics in Applied Earth Observations and Remote Sensing 11*(9), 3179–3195. https://doi.org/10.1109/JSTARS.2018.2824354

Schiewe, J. (2002). Segmentation of high-resolution remotely sensed data-concepts, applications and problems. *International Archives of Photogrammetry Remote Sensing and Spatial Information Sciences 34*(4), 380-385.

Shepherd, J. D., Bunting, P., & Dymond, J. R. (2019). Operational large-scale segmentation of imagery based on iterative elimination. *Remote Sensing 11*(6), 658. https://doi.org/10.3390/rs11060658

Singh, A. (1989). Review article digital change detection techniques using remotely sensed data. *International Journal of Remote Sensing 10*(6), 989–1003. https://doi.org/10.1080/01431168908903939

Singh, P. P., & Garg, R. D. (2011). Land use and land cover classification using satellite imagery: a hybrid classifier and neural network approach. *International Conference on Advances in Modeling, Optimization and Computing (AMOC)*, 753-762.

Singh, P. P. & Garg, R. D. (2014). Classification of high resolution satellite image using spatial constraints based fuzzy clustering. *Journal of Applied Remote Sensing 8*(1), 083526(1-16). https://doi.org/10.1117/1.JRS.8.083526

Stefanski, J., MacK, B., & Waske, O. (2013). Optimization of object-based image analysis with random forests for land cover mapping. *IEEE Journal of Selected Topics in Applied Earth Observations and Remote Sensing 6*(6), 2492–2504. https://doi.org/10.1109/JSTARS.2013.2253089

Thanh Noi, P., & Kappas, M. (2018). Comparison of random forest, k-nearest neighbor, and support vector machine classifiers for land cover classification using Sentinel-2 imagery. *Sensors 18*(1), 18. https://doi.org/10.3390/s18010018

Walter, V. (2004). Object-based classification of remote sensing data for change detection. *ISPRS Journal of photogrammetry and remote sensing 58*(3-4), 225-238. https://doi.org/10.1016/j.isprsjprs.2003.09.007

Wang, C., & Lu, L. (2019). Object-based random forest classification for detecting plastic-mulched landcover from Gaofen-2 and Landsat-8 OLI fused data. *8th International Conference on Agro-Geoinformatics, Agro-Geoinformatics* 1–5. https://doi.org/10.1109/Agro-Geoinformatics.2019.8820632

Wang, S. W., Gebru, B. M., Lamchin, M., Kayastha, R. B., & Lee, W. K. (2020). Land use and land cover change detection and prediction in the kathmandu district of nepal using remote sensing and GIS. *Sustainability (Switzerland) 12*(9). https://doi.org/10.3390/su12093925

Wang, X., Liu, S., Du, P., Liang, H., Xia, J., & Li, Y. (2018). Object-based change detection in urban areas from high spatial resolution images based on multiple features and ensemble learning. *Remote Sensing 10*(2). https://doi.org/10.3390/rs10020276

Weih, R. C., & Riggan, N. D. (2010). Object-based classification vs. pixel-based classification: Comparative importance of multi-resolution imagery. *The International Archives of the Photogrammetry, Remote Sensing and Spatial Information Sciences 38*(4), C7. DOI:10.4236/ars.2016.54022

Wu, J., Li, B., Ni, W., Yan, W., & Zhang, H. (2020). Optimal Segmentation Scale Selection for Object-Based Change Detection in Remote Sensing Images Using Kullback-Leibler Divergence. *IEEE Geoscience and Remote Sensing Letters 17*(7), 1124–1128. https://doi.org/10.1109/LGRS.2019.2943406

Zhang, Y., Peng, D., & Huang, X. (2018). Object-based change detection for VHR images based on multiscale uncertainty analysis. *IEEE Geoscience and Remote Sensing Letters 15*(1), 13–17. https://doi.org/10.1109/LGRS.2017.2763182